

DNA Plasticity Is a Key Determinant of the Energetics of Binding of Jun-Fos Heterodimeric Transcription Factor to Genetic Variants of TGACGTCA Motif[†]

Kenneth L. Seldeen, Caleb B. McDonald, Brian J. Deegan, Vikas Bhat, and Amjad Farooq*

Department of Biochemistry and Molecular Biology and USylvester Braman Family Breast Cancer Institute, Leonard Miller School of Medicine, University of Miami, Miami, Florida 33136

Received August 10, 2009; Revised Manuscript Received November 16, 2009

ABSTRACT: The Jun-Fos heterodimeric transcription factor is a target of a diverse array of signaling cascades that initiate at the cell surface and converge in the nucleus and ultimately result in the expression of genes involved in a multitude of cellular processes central to health and disease. Here, using isothermal titration calorimetry in conjunction with circular dichroism, we report the effect of introducing single nucleotide variations within the TGACGTCA canonical motif on the binding of bZIP domains of Jun-Fos heterodimer to DNA. Our data reveal that the Jun-Fos heterodimer exhibits differential energetics in binding to such genetic variants in the physiologically relevant micromolar to submicromolar range with the TGACGTCA canonical motif affording the highest affinity. Although binding energetics are largely favored by enthalpic forces and accompanied by entropic penalty, neither the favorable enthalpy nor the unfavorable entropy correlates with the overall free energy of binding in agreement with the enthalpy–entropy compensation phenomenon widely observed in biological systems. However, a number of variants including the TGACGTCA canonical motif bind to the Jun-Fos heterodimer with high affinity through having overcome such enthalpy–entropy compensation barrier, arguing strongly that better understanding of the underlying invisible forces driving macromolecular interactions may be the key to future drug design. Our data also suggest that the Jun-Fos heterodimer has a preference for binding to TGACGTCA variants with higher AT content, implying that the DNA plasticity may be an important determinant of protein–DNA interactions. This notion is further corroborated by the observation that the introduction of genetic variations within the TGACGTCA motif allows it to sample a much greater conformational space. Taken together, these new findings further our understanding of the role of DNA sequence and conformation on protein–DNA interactions in thermodynamic terms.

Transcription factors present the terminal link between the transfer of extracellular information in the form of growth factors and cytokines to the site of DNA transcription within the nucleus in a wide variety of cellular processes central to health and disease. This feat is in part executed by virtue of transcription factors to bind to specific recognition sites, termed response elements, within the promoters of target genes. Although such response elements are envisioned to comprise of a canonical sequence, typically spanning between 6 and 10 consecutive nucleotides, the promoters of many target genes in essence contain genetic variations of these response elements, and in particular, single nucleotide variants are extremely common within the eukaryotic genomes. Given that the nucleotide sequence is a key determinant of the ability of DNA to behave as a flexible polymer and undergo physical phenomena such as bending, stretching, deformation, and distortion coupled with its ability to exist in various structural conformations (such as the B-DNA, A-DNA, and Z-DNA) (1–3), our knowledge of how

genetic variations within the response elements influence the ability of transcription factors to bind and subsequently affect gene transcription remains largely elusive. In an attempt to embark on this challenge, our earlier work indicated that the single nucleotide variants (SNVs)¹ of the TGACTCA response element tightly modulate energetics and orientation of binding of the Jun-Fos heterodimeric transcription factor with important consequences on the recruitment of other cellular factors necessary for transcriptional machinery (4).

Jun-Fos heterodimer belongs to the AP1 (activator protein 1) family of transcription factors involved in executing the terminal stage of many critical signaling cascades that initiate at the cell surface and reach their climax in the nucleus (5–7). Upon activation by MAP kinases, AP1 binds to the promoters of a multitude of genes as Jun-Jun homodimer or Jun-Fos heterodimer. In so doing, Jun and Fos recruit the transcriptional machinery to the site of DNA and switch on expression of genes involved in a diverse array of cellular processes such as cell growth and proliferation, cell cycle regulation, embryonic development, and cancer (8–11). Jun and Fos recognize the two closely related canonical TGACTCA and TGACGTCA

[†]This work was supported by funds from the National Institutes of Health (Grant R01-GM083897), the American Heart Association (Grant 0655087B), and the USylvester Braman Family Breast Cancer Institute to A.F. C.B.M. is a recipient of a postdoctoral fellowship from the National Institutes of Health (Award T32-CA119929). B.J.D. and A.F. are members of the Sheila and David Fuente Graduate Program in Cancer Biology at the Sylvester Comprehensive Cancer Center of the University of Miami.

*To whom correspondence should be addressed: e-mail, amjad@farooqlab.net; tel, 305-243-2429; fax, 305-243-3955.

¹Abbreviations: AP1, activator protein 1; BR, basic region; His, polyhistidine tag; ITC, isothermal titration calorimetry; LZ, leucine zipper; MAP, mitogen-activated protein; PAGE, polyacrylamide gel electrophoresis; SDS, sodium dodecyl sulfate; SNP, single nucleotide polymorphism; SNV, single nucleotide variant; Trx, thioredoxin; bZIP, basic zipper.

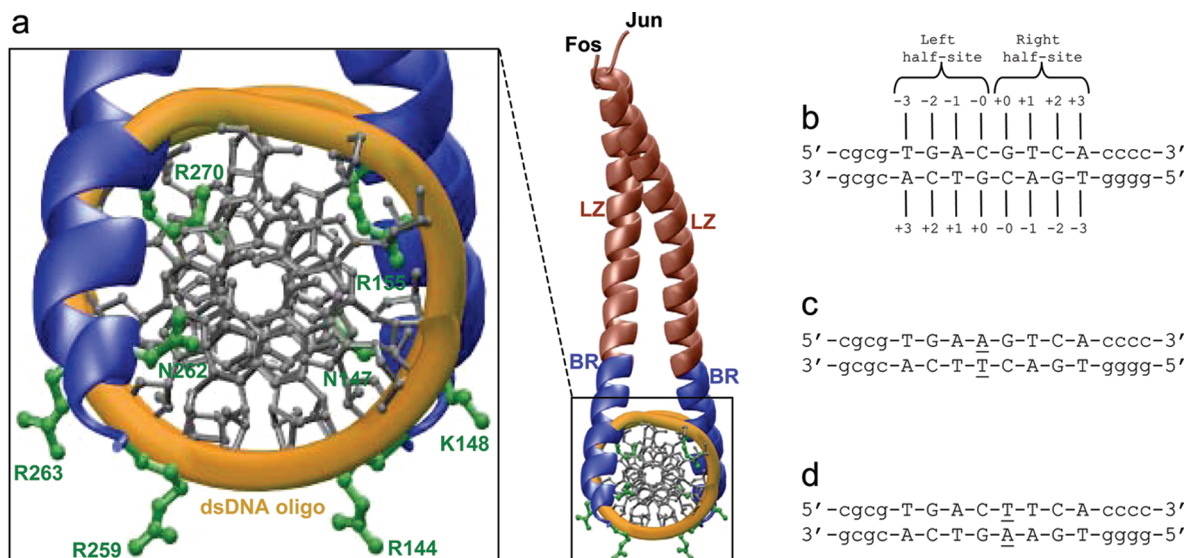


FIGURE 1: Protein and DNA analysis. (a) 3D structural representation of Jun-Fos heterodimer in complex with dsDNA oligo containing the TGACGTCA motif. The leucine zipper (LZ) and basic region (BR) domains are shown in brown and blue, respectively. Within the dsDNA oligo, the backbone is colored yellow and the bases are in gray. The side chain atoms of key amino acid residues involved in protein-DNA interaction are shown in green. The 3D atomic model shown was built as described previously (37). (b) Nucleotide sequence of 16-mer dsDNA oligo containing the TGACGTCA motif. The TGACGTCA motif is capitalized while the flanking nucleotides are shown in lower case letters. The numbering of various nucleotides relative to the central CG/GC base pairs (respectively assumed to be -0 and +0) in both strands is indicated. The TGAC and GTCA half-sites within this motif are also marked. (c) Nucleotide sequence of dsDNA oligo containing the C → A substitution at -0 position and herein referred to as the A-0 oligo. The variant nucleotides in both strands are underlined. (d) Nucleotide sequence of dsDNA oligo containing the G → T substitution at +0 position and herein referred to as the T+0 oligo. The variant nucleotides in both strands are underlined. Note that the A-0 and T+0 oligos shown in (c) and (d) are an example of a pair of symmetrically related dsDNA oligos, whereby the upper strand of one dsDNA oligo is identical to the lower strand of the other within the TGACGTCA sequence: they are indistinguishable upon the rotation of the variant motif by 180° in the plane of the paper (2-fold symmetry).

response elements, respectively referred to as the TPA (12-*O*-tetradecanoylphorbol 13-acetate) response element (TRE) and the cAMP response element (CRE), within the promoters of target genes through their so-called basic zipper (bZIP) domains (Figure 1a). The bZIP domain can be further dissected into two well-defined functional subdomains termed the basic region (BR) at the N-terminus followed by the leucine zipper (LZ) at the C-terminus. The leucine zipper is a highly conserved protein module found in a wide variety of cellular proteins and usually contains a signature leucine at every seventh position within the five successive heptads of amino acid residues. The leucine zippers adapt continuous α -helices in the context of Jun-Jun homodimer or Jun-Fos heterodimer by virtue of their ability to wrap around each other in a coiled-coil dimer (7, 12, 13). Such intermolecular arrangement brings the basic regions at the N-termini of bZIP domains into close proximity and thereby enables them to insert into the major grooves of DNA at the promoter regions in an optimal fashion in a manner akin to a pair of forceps (13). While the α -helices are held together by numerous interhelical hydrophobic contacts and salt bridges, hydrogen bonding between the side chains of basic residues in the basic regions and the DNA bases accounts for high-affinity binding of bZIP domains to DNA.

In an effort to further expand on our earlier efforts (4), we employ here isothermal titration calorimetry (ITC) in conjunction with circular dichroism (CD) to shed light on the effect of introducing single nucleotide variations within the TGACGTCA response element on the binding of Jun-Fos heterodimer to DNA. Such genetic variations are widely encountered in the promoters of a diverse array of genes under the control of AP1 transcription factor (14–36). Our new findings suggest that the genetic variations within the TGACGTCA canonical motif are an important determinant of DNA plasticity and that such

conformational flexibility may in turn intimately dictate the affinity of protein-DNA interactions central to gene transcription and regulation. Taken together, these new findings further our understanding of the role of DNA sequence and conformation on protein-DNA interactions in thermodynamic terms.

MATERIALS AND METHODS

Protein Preparation. bZIP domains of human Jun and Fos were cloned and expressed as described previously (4, 37). Briefly, the proteins were cloned into pET102 bacterial expression vector, with an N-terminal thioredoxin (Trx) tag and a C-terminal polyhistidine (His) tag, using Invitrogen TOPO technology. Additionally, thrombin protease sites were introduced at both the N- and C-termini of the proteins to aid in the removal of tags after purification. Proteins were subsequently expressed in *Escherichia coli* Rosetta2(DE3) bacterial strain (Novagen) and purified on a Ni-NTA affinity column using standard procedures. Further treatment of bZIP domains of Jun and Fos on a Hiload Superdex 200 size-exclusion chromatography (SEC) column coupled to a GE Akta FPLC system led to purification of recombinant domains to apparent homogeneity as judged by SDS-PAGE analysis. The identity of recombinant proteins was confirmed by MALDI-TOF mass spectrometry analysis. Final yields were typically between 10 and 20 mg of protein of apparent homogeneity per liter of bacterial culture. As noted previously (37), the treatment of recombinant proteins with thrombin protease significantly destabilized the bZIP domains of both Jun and Fos, and both domains appeared to be proteolytically unstable. For this reason, all experiments reported herein were carried out on recombinant fusion bZIP domains of Jun and Fos containing a Trx tag at the N-terminus and a His tag at the

C-terminus. The tags were found to have no effect on the binding of these domains to DNA under all conditions used here. Protein concentrations were determined as described earlier (37). Jun-Fos bZIP heterodimers were generated by mixing equimolar amounts of the purified bZIP domains of Jun and Fos. The efficiency of bZIP heterodimerization was close to 100% as judged by native PAGE and SEC analysis.

DNA Synthesis. The 16-mer DNA oligos containing the TGACGTCA consensus motif and all possible single nucleotide variants thereof were commercially obtained from Sigma Genosys. The flanking nucleotides were appropriately chosen to prevent self-annealing and to favor the formation of heteroduplexes from sense and antisense strands. The design of such oligos and the numbering of various nucleotides relative to the central CG bases are depicted in Figure 1b–d. Oligo concentrations were determined spectrophotometrically on the basis of their extinction coefficients derived from their nucleotide sequences using the online software OligoAnalyzer 3.0 (Integrated DNA Technologies) based on the nearest-neighbor model (38). Double-stranded DNA (dsDNA) oligos were generated as described earlier (37). Annealed dsDNA oligos were verified using native PAGE and circular dichroism (CD) analysis.

ITC Measurements. Isothermal titration calorimetry (ITC) experiments were performed on a Microcal VP-ITC instrument, and data were acquired and processed using Microcal ORIGIN software. All measurements were repeated two to three times. Briefly, the bZIP domains of Jun-Fos heterodimer and dsDNA oligos were prepared in 50 mM Tris, 200 mM NaCl, 1 mM EDTA, and 5 mM β -mercaptoethanol at pH 8.0. The experiments were initiated by injecting $25 \times 10 \mu\text{L}$ aliquots of 50–100 μM dsDNA oligo from the syringe into the calorimetric cell containing 1.8 mL of 5–10 μM bZIP domains of Jun-Fos heterodimer at 25 °C. The data were fit to a one-site model derived from the binding of a ligand to a macromolecule using the law of mass action to extract the various thermodynamic parameters as described previously (37). To ensure that the Trx and His tags did not interfere with the binding of DNA to Jun-Fos heterodimer, control experiments were conducted. Titration of a protein construct containing thioredoxin with a C-terminal His tag (Trx-His) in the calorimetric cell with dsDNA oligos in the syringe produced no observable signal, implying that the tags do not interact with DNA. In a similar manner, titration of bZIP domains of Jun-Fos heterodimer in the calorimetric cell with Trx-His construct in the syringe produced no observable signal, implying that the tags do not interact with bZIP domains. Additionally, the fact that the affinities obtained for the binding of bZIP domains of Jun-Fos heterodimer to dsDNA oligos containing the CRE site are in an excellent agreement with those reported previously for nontagged bZIP domains suggests that the Trx and His tags do not interfere with protein–DNA interactions reported here (12, 39–42).

CD Analysis. Circular dichroism (CD) measurements were conducted on a Bio-Logic MOS450 spectrometer equipped with a CD accessory and thermostatically controlled with a water bath. All data were acquired and processed using the Biokine software. For each experiment, 10 μM dsDNA oligo containing the TGACGTCA motif or a single nucleotide variant thereof was pre-equilibrated with an equimolar amount of bZIP domains of Jun-Fos heterodimer in 50 mM Tris, 200 mM NaCl, 1 mM EDTA, and 5 mM β -mercaptoethanol at pH 8.0. CD spectra were collected at 25 °C using a quartz cuvette with a 2 mm path length in the wavelength range 200–300 nm and normalized

against a reference spectrum to remove the contribution of protein to DNA ellipticity. The reference spectrum was obtained in a similar manner on a 10 μM solution of bZIP domains of Jun-Fos heterodimer in the same buffer. Data were recorded with a slit bandwidth of 2 nm at a scan rate of 3 nm/min. Each data set represents an average of two to three scans acquired at 1 nm intervals.

RESULTS AND DISCUSSION

Single Nucleotide Variants of the TGACGTCA Motif Dictate the Energetics of Binding of Jun-Fos Heterodimer. Given that they are widely encountered in the promoters of a diverse array of genes (14–36), addressing the issue of how single nucleotide variants of the TGACGTCA motif influence the binding of Jun-Fos heterodimer is of paramount interest. Figure 2 shows a set of representative ITC isotherms obtained for the TGACGTCA canonical motif and two variants. The complete thermodynamic profiles for the entire set of variants are provided in Table 1. It is clearly evident from our data that the Jun-Fos heterodimer binds to all TGACGTCA variants with physiologically relevant affinity in the micromolar to submicromolar range. Remarkably, the TGACGTCA canonical motif affords the most optimal affinity that is close to an order of magnitude stronger than the TGACTTCA variant, the sequence that is energetically least favorable for binding to the Jun-Fos heterodimer. Given its occurrence in the gene promoters with higher frequency combined with its higher affinity for binding to Jun-Fos heterodimer relative to other variants, the TGACGTCA canonical motif will be hereinafter referred to as the wild-type (WT) motif for the purpose of distinguishing it from other variants which have been assigned nomenclature according to the position of the nucleotide substitution (Table 1). It should also be noted here that the binding of all TGACGTCA variants to Jun-Fos heterodimer is largely driven by favorable enthalpic forces accompanied by unfavorable entropic penalty, an observation in agreement with the knowledge that protein–DNA interactions are predominantly driven by electrostatic interactions and hydrogen bonding. Comparison of these data with the binding of Jun-Fos heterodimer to nucleotide variants of the TGACTCA pseudopalindrome suggests that the nucleotide variations within the TGACGTCA palindrome display a much tighter binding window stretching just under 10-fold while it spanned over nearly 60-fold in the case of the pseudopalindrome (4). One likely scenario for the rather higher tolerance of the TGACGTCA palindrome to genetic variations in terms of its ability to bind to Jun-Fos heterodimer relative to the TGACTCA pseudopalindrome may be due to the larger separation of the TGA and TCA half-sites within the palindrome and thereby allowing the protein greater freedom to slide between these half-sites in response to specific genetic changes. Although the role of sliding is not strange to protein–DNA interactions (43–46), further studies are clearly warranted to assess the extent to which the ability of Jun-Fos heterodimer to slide along its response elements within the promoters of target genes may factor into its energetics of binding.

Jun-Fos Heterodimer Binds to All Possible Single Nucleotide Variants of the TGACGTCA Motif without a Preferred Orientation. In a previous study, we reported that certain variants of the TGACTCA motif result in the binding of Jun-Fos heterodimer with a preferred orientation due to the ability of each monomer to engage in asymmetric protein–DNA

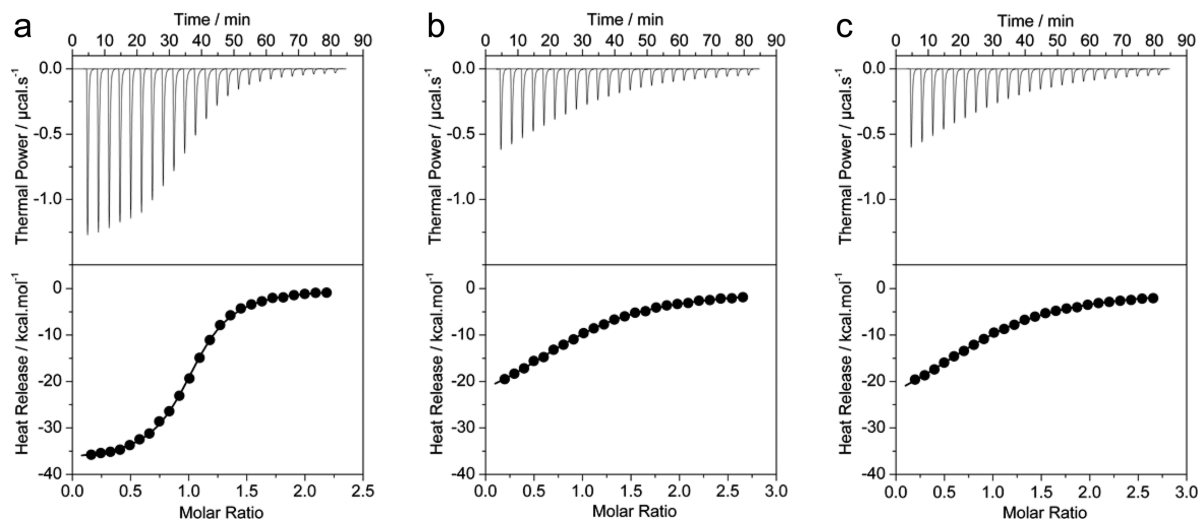


FIGURE 2: Representative ITC isotherms for the binding of bZIP domains of Jun-Fos heterodimer to dsDNA oligos containing the promoter sites TGACGTCA (a), TGAAGTCA (b), and TGACTTCA (c). In each case, 8 μ M dimer equivalent of bZIP domains in the calorimetric cell was titrated with 100 μ M corresponding dsDNA oligo in the syringe. The upper panels show the raw ITC data expressed as change in thermal power with respect to time over the period of titration. In the lower panels, change in molar heat is expressed as a function of molar ratio of dsDNA oligos to Jun-Fos heterodimer. The solid lines represent the fit of data points in the lower panels to a function based on the binding of a ligand to a macromolecule using the Microcal ORIGIN software (68). All data are shown to the same scale for direct comparison. Note that the variant motif TGAAGTCA is related to the TGACTTCA motif by 2-fold symmetry. The position of the variant nucleotide in each of the sites relative to the consensus sequence TGACGTCA is underlined.

Table 1: Experimentally Determined Thermodynamic Parameters for the Binding of bZIP Domains of Jun-Fos Heterodimer to dsDNA Oligos Containing the Wild-Type (WT) TGACGTCA Canonical Motif and All Possible Single Nucleotide Variants Thereof Obtained from ITC Measurements at 25 °C and pH 8.0^a

motif	sequence	<i>n</i>	<i>K_d</i> /μM	ΔH /kcal mol ⁻¹	$T\Delta S$ /kcal mol ⁻¹	ΔG /kcal mol ⁻¹	gene promoter
WT	TGACGTCA	1.00 ± 0.02	0.27 ± 0.01	-37.22 ± 0.05	-28.25 ± 0.04	-8.96 ± 0.01	peptide hormone somatostatin
A-3	<u>A</u> GACGTCA	1.01 ± 0.02	1.75 ± 0.07	-30.50 ± 0.18	-22.63 ± 0.15	-7.86 ± 0.02	reproductive regulator GnRh II
C-3	<u>C</u> GACGTCA	0.99 ± 0.02	1.52 ± 0.04	-33.58 ± 0.12	-25.61 ± 0.11	-7.94 ± 0.02	neuropeptide YY1 receptor
G-3	<u>G</u> GACGTCA	0.98 ± 0.03	2.32 ± 0.03	-33.09 ± 0.08	-25.37 ± 0.11	-7.69 ± 0.01	cytokine IL-6
A-2	T <u>A</u> ACGTCA	1.07 ± 0.03	1.16 ± 0.07	-30.34 ± 0.20	-22.23 ± 0.17	-8.10 ± 0.03	cyclin D1
C-2	T <u>C</u> ACGTCA	0.94 ± 0.04	1.01 ± 0.01	-37.47 ± 0.12	-29.25 ± 0.15	-8.19 ± 0.01	cytokine IL-12b
T-2	T <u>T</u> ACGTCA	1.05 ± 0.01	0.44 ± 0.01	-34.01 ± 0.12	-25.33 ± 0.13	-8.68 ± 0.01	metabolic enzyme PEPCK
C-1	TG <u>C</u> CGTCA	1.06 ± 0.01	1.88 ± 0.11	-33.40 ± 0.13	-25.58 ± 0.11	-7.82 ± 0.03	endocrine hormone TRH
G-1	TG <u>G</u> CGTCA	0.98 ± 0.06	1.37 ± 0.15	-32.24 ± 0.38	-24.23 ± 0.34	-8.01 ± 0.06	DNA clamp PCNA
T-1	TG <u>T</u> CGTCA	0.94 ± 0.03	1.18 ± 0.01	-38.45 ± 0.02	-30.36 ± 0.03	-8.09 ± 0.01	glycoprotein hormone α2
A-0	TGA <u>A</u> GTCA	0.96 ± 0.02	2.41 ± 0.03	-28.73 ± 0.22	-21.04 ± 0.21	-7.67 ± 0.01	protein kinase Cδ
G-0	TGA <u>G</u> GTCA	1.01 ± 0.02	2.17 ± 0.14	-33.45 ± 0.08	-25.69 ± 0.13	-7.73 ± 0.04	surfactant protein B
T-0	TGA <u>T</u> GTCA	0.95 ± 0.01	0.95 ± 0.03	-32.93 ± 0.06	-24.67 ± 0.04	-8.22 ± 0.02	transglutaminase TGM1
A+0	TGAC <u>A</u> TCA	1.04 ± 0.02	0.80 ± 0.01	-30.36 ± 0.21	-22.02 ± 0.21	-8.33 ± 0.01	neurotensin peptide NT
C+0	TGAC <u>C</u> TCA	0.97 ± 0.01	1.61 ± 0.02	-33.10 ± 0.02	-25.20 ± 0.02	-7.91 ± 0.01	extracellular glycoprotein OPN
T+0	TGAC <u>T</u> TCA	0.91 ± 0.02	2.66 ± 0.06	-30.43 ± 0.11	-22.83 ± 0.08	-7.61 ± 0.01	parathyroid-like hormone PTHrP
A+1	TGAC <u>G</u> ACA	1.00 ± 0.06	1.32 ± 0.10	-32.52 ± 0.32	-24.48 ± 0.27	-8.03 ± 0.04	motor neuron protein SMN2
C+1	TGAC <u>G</u> CCA	1.05 ± 0.01	1.41 ± 0.02	-32.42 ± 0.18	-24.44 ± 0.17	-7.99 ± 0.01	serotonin N-acetyltransferase NAT
G+1	TGAC <u>G</u> GCA	0.95 ± 0.03	1.85 ± 0.03	-35.45 ± 0.13	-27.61 ± 0.11	-7.83 ± 0.01	interferon regulator IRF1
A+2	TGACG <u>T</u> AA	1.06 ± 0.01	0.51 ± 0.02	-29.68 ± 0.13	-21.08 ± 0.15	-8.59 ± 0.02	gastric protein chromogranin A
G+2	TGACG <u>T</u> GA	1.02 ± 0.04	1.53 ± 0.07	-31.09 ± 0.14	-23.14 ± 0.11	-7.94 ± 0.03	NMDA receptor subunit NR2B
T+2	TGACG <u>T</u> TA	0.96 ± 0.04	1.24 ± 0.13	-30.97 ± 0.42	-22.90 ± 0.36	-8.07 ± 0.06	apoptotic repressor BCL2
C+3	TGACGT <u>C</u> C	0.95 ± 0.01	1.91 ± 0.05	-30.70 ± 0.06	-22.89 ± 0.08	-7.81 ± 0.02	histone H4
G+3	TGACGT <u>C</u> G	0.99 ± 0.04	1.83 ± 0.05	-32.20 ± 0.12	-24.36 ± 0.15	-7.84 ± 0.02	ornithine decarboxylase ODC
T+3	TGACGT <u>T</u> T	1.00 ± 0.05	1.30 ± 0.03	-28.95 ± 0.21	-20.90 ± 0.23	-8.04 ± 0.02	superoxide dismutase MnSOD

^aNote that the DNA sequence shown for the TGACGTCA motif and its single nucleotide variants corresponds to the sense strand only, and nucleotides flanking these motifs have been omitted for clarity (see Figures 1b–d). The substituted nucleotide relative to the TGACGTCA motif is underlined. One example of a gene promoter that contains a particular TGACGTCA variant for recruiting the AP1 transcription factor is provided for physiological relevance (14–36). The values for the stoichiometry (*n*), affinity (*K_d*), and enthalpy change (ΔH) accompanying the binding of bZIP domains of Jun-Fos heterodimer to dsDNA oligos were obtained from the fit of a function, based on the binding of a ligand to a macromolecule using the law of mass action (68), to the ITC isotherms. Free energy of binding (ΔG) was calculated from the relationship $\Delta G = RT \ln K_d$, where *R* is the universal molar gas constant (1.99 cal mol⁻¹ K⁻¹) and *T* is the absolute temperature (K). Entropic contribution ($T\Delta S$) to binding was calculated from the relationship $T\Delta S = \Delta H - \Delta G$. Errors were calculated from two to three independent measurements. Three measurements were carried out for all motifs but those with the substitutions at zero positions (-0 and +0). All errors are given to one standard deviation.

contacts (4). In an attempt to assess the extent to which the Jun-Fos heterodimer might be able to display such orientational

preference in complex with TGACGTCA variants, we constructed a plot showing the relative binding of symmetrically

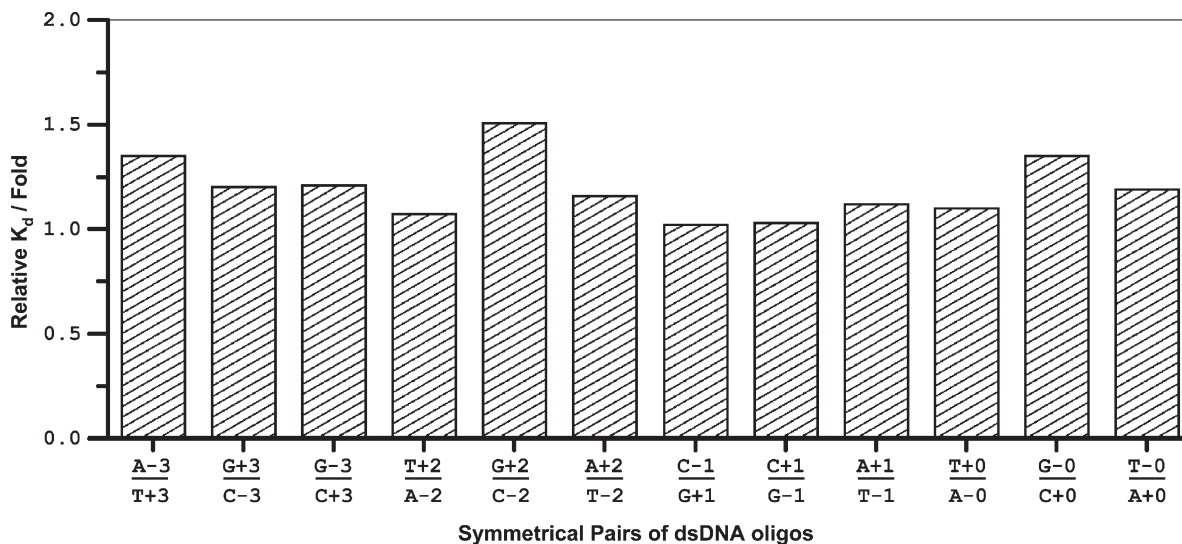


FIGURE 3: Analysis of relative binding of symmetrically related pairs of dsDNA oligos containing TGACGTCA variants to bZIP domains of Jun-Fos heterodimer. Relative binding is defined as the ratio of the K_d of the binding of one dsDNA oligo to Jun-Fos heterodimer over that of the other. The nomenclature for the various dsDNA oligos shown is the same as that indicated in Table 1.

related pairs of TGACGTCA variants to Jun-Fos heterodimer (Figure 3). Note that the symmetrically related pairs of TGACGTCA variants are related by a 2-fold symmetry, whereby the upper strand of one dsDNA oligo is identical to the lower strand of the other within the TGACGTCA sequence. Given such symmetrical relationship, one would expect the binding of Jun-Fos heterodimer to symmetrically related pairs of TGACGTCA variants to be energetically equivalent and thus result in indistinguishable affinities. The only exception to this rule would arise if the two monomers were not able to exchange freely due to nonequivalent contacts with flanking nucleotides in one strand over the other. Such asymmetric binding would be expected to result in a preferred orientation of Jun-Fos heterodimer to the specific TGACGTCA variants. As shown in Figure 3, our data reveal that the Jun-Fos heterodimer binds to all TGACGTCA variants with relative K_d values close to unity, implying that the binding largely occurs via nonpreferred orientation due to little or negligible differences in the energetics of binding. The small deviations from unity in the values of relative K_d could be accounted for by the differences in the flanking nucleotides for the symmetrically related pairs of TGACGTCA variants. Whether such small differences in the binding energetics could be sufficient to orient the Jun-Fos heterodimer clearly warrants further studies. It should be noted however that the orientation of transcription factors in complex with DNA plays a critical role in defining the nature of other cellular factors that can be recruited to the site of DNA transcription in a temporal and spatial manner. In this context, the possibility that the Jun-Fos heterodimer may bind in an oriented manner to some TGACGTCA variants cannot be ruled out on the basis of data presented herein.

High-Affinity Binding of the TGACGTCA Motif Is in Part Owed to Overcoming the Enthalpy–Entropy Compensation Barrier. Enthalpy–entropy compensation is a phenomenon that is widely observed in biological systems (47–51). In a nutshell, it postulates that enthalpic contributions to macromolecular interactions are compensated by equal but opposing entropic changes such that there is no net gain in the overall free energy. Figure 4 shows the enthalpy–entropy compensation plot for the binding of TGACGTCA canonical motif and all single nucleotide variants thereof to Jun-Fos

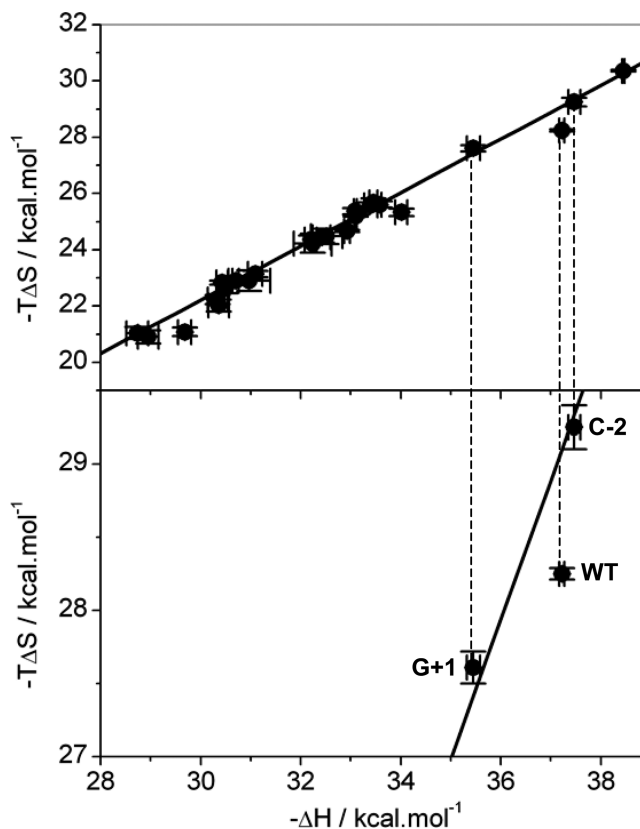


FIGURE 4: Enthalpy (ΔH)–entropy ($T\Delta S$) plot for the binding of TGACGTCA variants to Jun-Fos heterodimer. The top panel shows the ΔH – $T\Delta S$ plot for the binding of Jun-Fos heterodimer to all possible single nucleotide variants of the TGACGTCA motif. The bottom panel shows an expanded view of WT oligo (that appears to have defeated the enthalpy–entropy compensation barrier) flanked between G+1 and C-2 variants (that faithfully obey the enthalpy–entropy compensation phenomenon) on the ΔH – $T\Delta S$ plot. The solid lines represent linear fits to the data in the top panel. Error bars were calculated from two to three independent measurements. All error bars are given to one standard deviation. The nomenclature for the various oligos is the same as that indicated in Table 1.

heterodimer. It should be noted however that the enthalpy–entropy compensation is not an absolute thermodynamic law nor

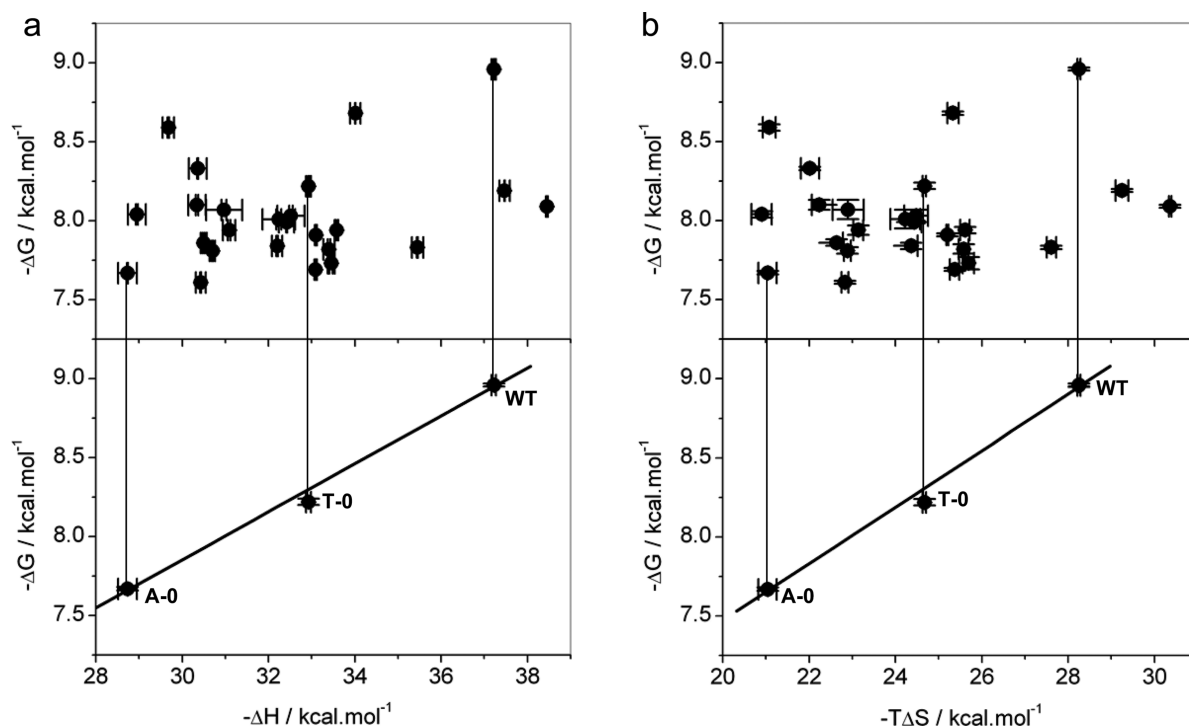


FIGURE 5: Dependence of enthalpic (ΔH) and entropic ($T\Delta S$) contributions to the free energy (ΔG) of binding of TGACGTCA variants to Jun-Fos heterodimer. (a) The upper panel shows the ΔH – ΔG plot for the binding of Jun-Fos heterodimer to all possible single nucleotide variants of the TGACGTCA motif. The lower panel shows a triplet of oligos (A-0, T-0, and WT) that follow the general trend of an increase in $-\Delta H$ correlating with an increase in $-\Delta G$. (b) The upper panel shows the $T\Delta S$ – ΔG plot for the binding of Jun-Fos heterodimer to all possible single nucleotide variants of the TGACGTCA motif. The lower panel shows a triplet of oligos (A-0, T-0, and WT) that follow the general trend of an increase in $-\Delta G$ correlating with an increase in $-\Delta G$. Note that the solid lines represent linear fits to the data shown in each panel. Error bars were calculated from two to three independent measurements. All error bars are given to one standard deviation. The nomenclature for the various oligos is the same as that indicated in Table 1.

it ought to be obeyed universally. Indeed, if it were to be obeyed, macromolecular interactions would be expected to be of similar affinity across the board in lieu of ranging from weak interactions in the micromolar range to ultratight interactions in the picomolar range observed in diverse cellular processes. Supporting these arguments, enthalpy–entropy compensation plot for the binding of Jun-Fos heterodimer to TGACGTCA variants suggests that a number of motifs, including the TGACGTCA canonical motif, indeed overcome the enthalpy–entropy barrier to bind with affinities much higher than would have been possible otherwise (Figure 4). Close scrutiny of the thermodynamics of TGACGTCA canonical motif suggests that it somehow manages to release about -1 kcal/mol of favorable enthalpy without paying anything for it in entropy penalty upon binding to the Jun-Fos heterodimer. Had it not been for such escape from enthalpy–entropy compensation, the binding of TGACGTCA canonical motif to Jun-Fos heterodimer would have been reduced to an affinity in the micromolar range in lieu of the experimentally observed submicromolar range (Figure 4 and Table 1) and thereby rendering it one of the weakest variants to recognize the Jun-Fos heterodimer. The TGACGTCA (WT) canonical motif is immediately flanked between TGACGGCA (G+1) and TCACGTCA (C-2) variants on the enthalpy–entropy compensation plot (Figure 4, lower panel). Note that, unlike the WT motif, G+1 and C-2 motifs faithfully obey the enthalpy–entropy compensation. In comparison with G+1 and C-2 motifs, the ability of the WT motif to defeat the enthalpy–entropy compensation barrier must reside in its distinguishing chemistry at positions +1 and –2 that allows it to engage in intermolecular contacts that favor the release of

enthalpy but cause minimal changes in unfavorable entropy. Close scrutinization of 3D structure of Jun-Fos heterodimer in complex with DNA reveals that the nucleotides (or their complementary pairs) at +1 and –2 positions reside in the major groove and engage in hydrogen bonding with the side chain of N262 within the Jun monomer and the side chain of N147 within the Fos monomer, respectively (Figure 1a). It is thus conceivable that the distinguishing chemical nature of nucleotides at +1 and –2 positions within the WT motif versus the G+1 and C-2 variants could account for their distinguishing thermodynamic features. Although complete analysis of the underlying forces that allow the WT motif to escape the enthalpy–entropy barrier but not the G+1 and C-2 motifs is beyond the scope of this study, our data presented herein nonetheless provide a glimpse into the interacting forces that determine the overall binding affinity of protein–DNA interactions. Our data also argue strongly that the design of future drugs sporting greater efficacy coupled with low toxicity could benefit from the consideration of underlying thermodynamic forces.

Enthalpic and Entropic Contributions Do Not Correlate with the Energetics of Binding of Jun-Fos Heterodimer to TGACGTCA Variants. Given that protein–DNA interactions are usually driven by enthalpy accompanied by entropic penalty (52–57), we next asked the question whether there was any correlation between enthalpy and entropy versus the overall free energy for the binding of TGACGTCA variants to the Jun-Fos heterodimer. As illustrated in Figure 5, our data show that an increase in free energy correlates with neither favorable enthalpy nor favorable entropy in agreement with the enthalpy–entropy compensation phenomenon discussed above. In other

words, a small favorable enthalpy may be sufficient to generate a high binding affinity by virtue of a small corresponding entropic penalty. Conversely, a large favorable enthalpy does not necessarily result in tighter binding due to a compensating increase in entropic penalty. Despite the lack of such an overall correlation in the entire cohort of TGACGTCA variants (Figure 5, upper panels), we have identified a subset of variants that exquisitely display a correlation between enthalpy and entropy versus the free energy. These include the A-0, T-0, and WT motifs, whose favorable enthalpy and unfavorable entropy positively correlate with free energy enhancement in what would be referred to as “enthalpically optimized” variants (Figure 5, lower panels). Note that all of these motifs differ from each other in the nature of nucleotide at -0 position: WT motif is identical to A-0 and T-0 except for the presence of a cytosine at -0 position. What can we learn from such findings? It is clear that higher binding affinity is achievable through optimizing both the enthalpic and entropic contributions and thus overcoming the enthalpy–entropy compensation barrier that too often acts as a bottleneck to rationale drug design. In the case of A-0, T-0, and WT variants, optimization of enthalpic contribution results in an enhancement of binding affinity by nearly an order of magnitude from a value of $2.41 \mu\text{M}$ for the A-0 motif to a value of $0.27 \mu\text{M}$ for the WT motif (Table 1). Close analysis of the 3D structure of the Jun-Fos heterodimer in complex with DNA suggests that the nucleotides at -0 position and their complementary pairs on the opposite strand engage in hydrogen bonding with R270 within the Jun monomer and R155 within the Fos monomer (Figure 1a). In light of these observations, the most likely scenario for the increase in binding affinity as a direct result of an increase in favorable enthalpy for the A-0, T-0, and WT motifs is that the smaller thymine and cytosine bases instead of the larger adenine at the -0 position are enthalpically preferred. Taken together, our data provide precedence for the design of higher affinity ligands on thermodynamic grounds through optimization of enthalpic and entropic contributions. Although our data suggest that enthalpically optimized ligands may be more amenable to design, there is a growing school of thought that the future design of drugs could also benefit from favorable entropic contributions to the free energy in what has come to be termed as “entropically optimized drugs”.

A/T Substitutions Are Preferred over G/C Substitutions within the TGACGTCA Motif for Binding to Jun-Fos Heterodimer. It is widely believed that A/T sequences within DNA account for its intrinsic conformational flexibility such as bending and curvature (1, 2, 58–63). Such intrinsic propensity of A/T sequences to undergo bending is believed to be largely due to increased propeller twist of these sequences by virtue of the fact that A-T base pairs are held together by only two hydrogen bonds in lieu of three formed between G-C base pairs. In an attempt to analyze how single nucleotide substitutions of A/T versus G/C affect the binding of TGACGTCA variants to Jun-Fos heterodimer, we generated thermodynamic plots shown in Figure 6. It is immediately evident that G/C substitutions are enthalpically more favorable at all positions within the TGACGTCA motif but -1 and $+2$, presumably by virtue of their ability to engage in greater intermolecular contacts via hydrogen bonding and hydrophobic forces (Figure 6, top panel). In contrast, A/T substitutions are entropically more favorable at all positions within the TGACGTCA motif but -1 and $+1$, indicative of their intrinsic flexibility allowing them to engage in close intermolecular contacts (Figure 6, middle panel). Given the antagonistic

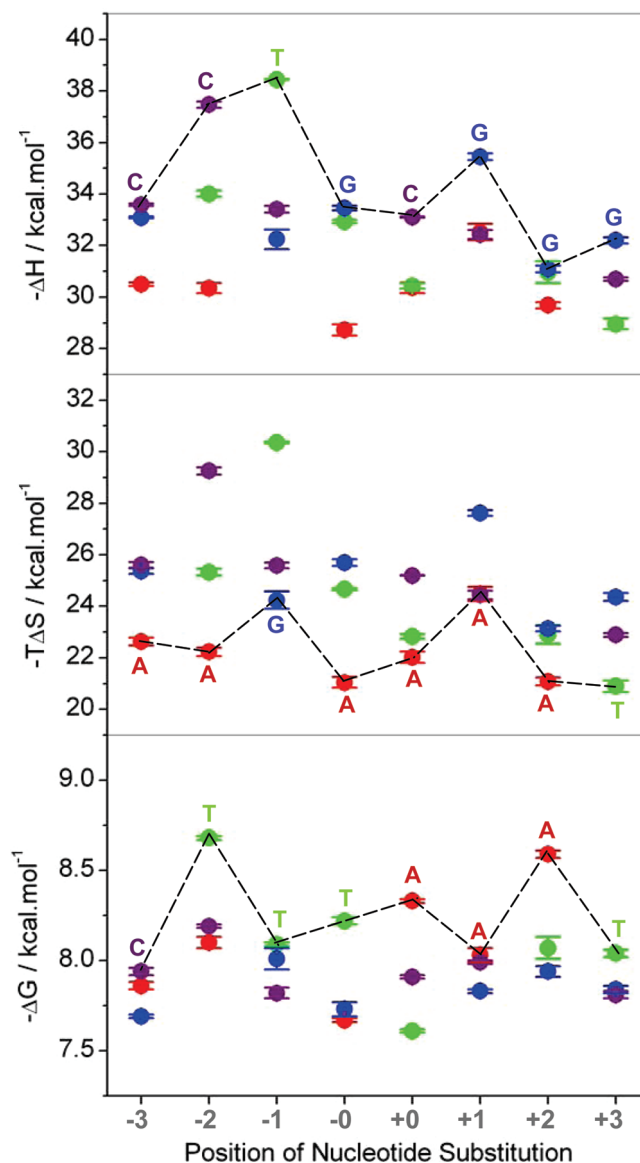


FIGURE 6: Dependence of enthalpy (ΔH), entropy ($T\Delta S$), and free energy (ΔG) on the position of nucleotide substitution within the TGACGTCA motif. The changes in various thermodynamic parameters upon the introduction of A, T, G, and C substitutions at various positions are respectively denoted by red, green, blue, and purple circles. The dashed line in the top panel connects the enthalpically most favorable nucleotide at each position within the TGACGTCA motif. The dashed line in the middle panel connects the entropically most favorable nucleotide at each position within the TGACGTCA motif. The dashed line in the bottom panel connects the overall energetically most favorable nucleotide at each position within the TGACGTCA motif. Error bars were calculated from two to three independent measurements. All error bars are given to one standard deviation. The nomenclature for the various oligos is the same as that indicated in Table 1.

actions of A/T and G/C substitutions on underlying thermodynamic forces, it might be inferred that the overall free energy of binding may not correlate with A/T or G/C substitutions at any one given position within the TGACGTCA motif. On the contrary, A/T substitutions are preferred at all positions but -3 for the optimal binding of Jun-Fos heterodimer (Figure 6, bottom panel). Taken together, these salient observations imply that the conformational plasticity such as the ability of TGACGTCA variants to bend and wrap around Jun and Fos to attain a close molecular fit is critical for high-affinity binding.

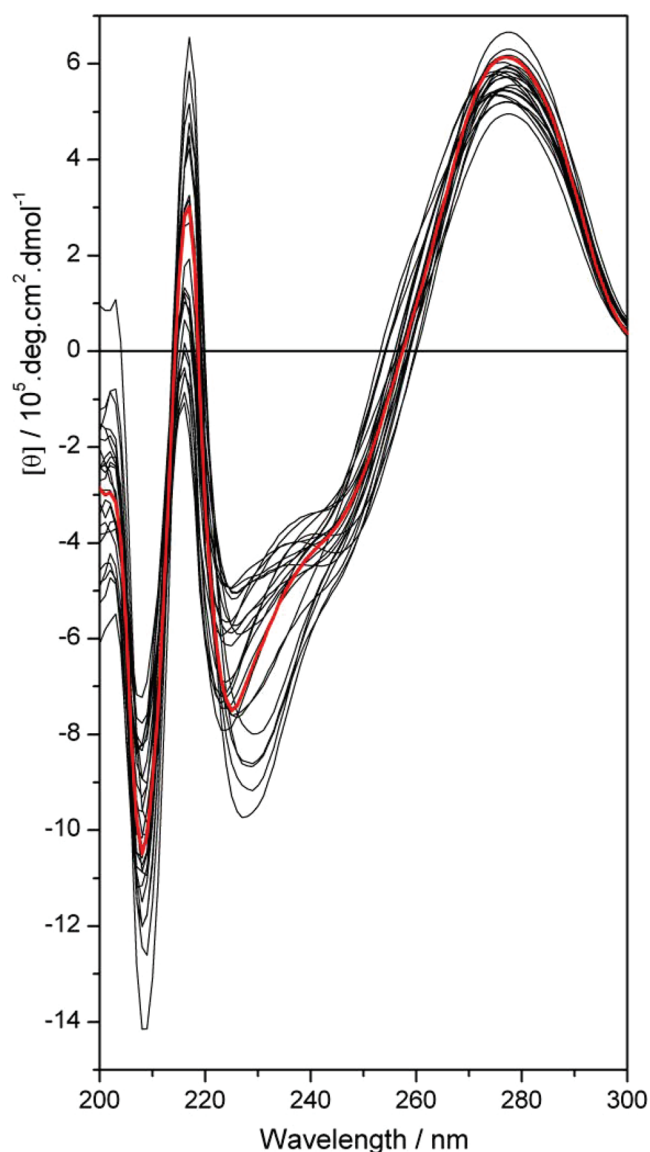


FIGURE 7: CD spectra of dsDNA oligos containing the TGACGTCA motif and all possible single nucleotide variants thereof bound to Jun-Fos heterodimer (with the protein contributions removed). The CD spectrum of the TGACGTCA motif (red) is superimposed upon CD spectra of all the other variants (black).

Although DNA bending is not observed in the crystal structure of Jun-Fos heterodimer bound to the related TGACTCA motif (13), several solution studies argue in support of the role of intrinsic bendability of DNA as being a key factor in its ability to bind to Jun-Fos heterodimer with high affinity (64–66).

DNA Conformational Flexibility Appears To Play a Key Role in the Differential Binding of TGACGTCA Variants to Jun-Fos Heterodimer. In light of the above observations coupled with the notion that the nucleotide sequence is a key determinant of the ability of DNA to behave as a flexible polymer and undergo physical phenomena such as bending and curvature (1–3), we further analyzed the conformational flexibility of the TGACGTCA motif and all the variants thereof in complex with Jun-Fos heterodimer by CD spectroscopy. As shown in Figure 7, the CD spectra of bound DNA (with the protein contributions largely removed) exhibit features characteristic of a right-handed double-stranded B-DNA with bands centered around 220 and 280 nm. It should be noted here that

while the 220 nm band arises from secondary structural DNA features, the 280 nm band probes the 3D conformation of DNA, and therefore it is highly sensitive to physical changes in DNA such as bending and curvature. It is clearly evident that the CD spectra of the variant oligos do not superimpose upon the CD spectrum of the TGACGTCA motif but rather fluctuate around it and fan out, forming a cluster of closely related optical spectra. This salient observation implies that the introduction of single nucleotide substitutions within the TGACGTCA motif tightly governs its conformational flexibility and that the varying flexibility is likely to be an integral feature of their ability to bind to Jun-Fos heterodimer with distinct underlying energetics. While the intensity of the 280 nm band is related to overall 3D conformation of DNA, it is not easily interpretable in structural terms such as bending and curvature. Nonetheless, our CD data indicate that the introduction of genetic variations within the TGACGTCA motif allows it to sample a much greater conformational space that might be a key feature of the ability of its variants to bind to the Jun-Fos heterodimer at distinct promoters in a selective manner.

CONCLUSIONS

Transcription factors play a central role in the transduction of cellular signals into gene expression via their ability to recognize DNA in a sequence-specific manner. The precise sequence of DNA determines its physical properties, such as bending and curvature, allowing it to adapt into a complementary shape to provide the best fit for the incoming protein partner (1–3). Our data presented herein indeed add to this school of thought. Our study shows that genetic variations within the TGACGTCA motif modulate energetics of binding of the Jun-Fos heterodimer by virtue of their ability to bend and curve accordingly to obtain the optimal molecular fit between the two interacting partners. The genetic variations within the response elements may thus play an important role in regulating the biological activity of Jun-Fos heterodimer at specific promoters. Our findings also bear important consequences for the occurrence of single nucleotide polymorphisms (SNPs) within promoter regions containing the AP1-responsive site. It has indeed been shown that a SNP that changes the TGACGTCA canonical motif to the TGACGTTA variant alters transcription factor binding (67). While many proteins bind to unperturbed DNA, the plasticity of the TGACGTCA variants appears to be a key feature of their ability to bind to Jun-Fos heterodimer on the basis of data reported herein and elsewhere (64–66). In particular, the content and position of A/T nucleotides within the TGACGTCA variants may be an important determinant of their ability to bend and deform upon binding. It is widely believed that A/T sequences within DNA account for its intrinsic conformational flexibility such as bending and curvature (1, 2, 58–63). These observations are further supported by our findings that A/T substitutions are preferred at all positions within the TGACGTCA motif but –3 for the optimal binding of Jun-Fos heterodimer, implying that the structural plasticity of DNA is necessary for high-affinity protein–DNA interactions. Our data also suggest that the TGACGTCA canonical motif defies the enthalpy–entropy compensation barrier in order to bind with a high affinity. Although the enthalpy–entropy compensation barrier is widely observed in biological systems and presents a bottleneck for the design of high-affinity drugs to combat disease, our findings clearly lay the groundwork for furthering our understanding of the invisible

forces driving macromolecular interactions and may lead to unlocking the secrets to overcoming this thermodynamic barrier for the design of next-generation drugs sporting greater efficacy coupled with low toxicity. The design of high-affinity ligands on thermodynamic grounds through optimization of enthalpic and entropic contributions may indeed be one of the major frontiers that we have to conquer to improve the clinical design of future therapies. In conclusion, the present study provides a comprehensive analysis of the effect of genetic variations within the TGACGTCA motif on the energetics of binding of Jun-Fos heterodimer. Our data strongly argue that such genetic variations control the plasticity and conformational deformability of the target DNA and thereby bear important consequences for the physiological role of this key transcription factor central to health and disease.

REFERENCES

- Marini, J. C., Levene, S. D., Crothers, D. M., and Englund, P. T. (1982) Bent helical structure in kinetoplast DNA. *Proc. Natl. Acad. Sci. U.S.A.* 79, 7664–7668.
- Wu, H. M., and Crothers, D. M. (1984) The locus of sequence-directed and protein-induced DNA bending. *Nature* 308, 509–513.
- Munteanu, M. G., Vlahovicek, K., Parthasarathy, S., Simon, I., and Pongor, S. (1998) Rod models of DNA: sequence-dependent anisotropic elastic modelling of local bending phenomena. *Trends Biochem. Sci.* 23, 341–347.
- Seldeen, K. L., McDonald, C. B., Deegan, B. J., and Farooq, A. (2009) Single nucleotide variants of the TGACTCA motif modulate energetics and orientation of binding of the Jun-Fos heterodimeric transcription factor. *Biochemistry* 48, 1975–1983.
- Chinenov, Y., and Kerppola, T. K. (2001) Close encounters of many kinds: Fos-Jun interactions that mediate transcription regulatory specificity. *Oncogene* 20, 2438–2452.
- Angel, P., and Karin, M. (1991) The role of Jun, Fos and the AP-1 complex in cell-proliferation and transformation. *Biochim. Biophys. Acta* 1072, 129–157.
- Curran, T., and Franz, B. R., Jr. (1988) Fos and Jun: the AP-1 connection. *Cell* 55, 395–397.
- Baxeianis, A. D., and Vinson, C. R. (1993) Interactions of coiled coils in transcription factors: where is the specificity? *Curr. Opin. Genet. Dev.* 3, 278–285.
- Raivich, G., and Behrens, A. (2006) Role of the AP-1 transcription factor c-Jun in developing, adult and injured brain. *Prog. Neurobiol.* 78, 347–363.
- Milde-Langosch, K. (2005) The Fos family of transcription factors and their role in tumorigenesis. *Eur. J. Cancer* 41, 2449–2461.
- Jochum, W., Passegue, E., and Wagner, E. F. (2001) AP-1 in mouse development and tumorigenesis. *Oncogene* 20, 2401–2412.
- Halazonetis, T. D., Georgopoulos, K., Greenberg, M. E., and Leder, P. (1988) c-Jun dimerizes with itself and with c-Fos, forming complexes of different DNA binding affinities. *Cell* 55, 917–924.
- Glover, J. N., and Harrison, S. C. (1995) Crystal structure of the heterodimeric bZIP transcription factor c-Fos-c-Jun bound to DNA. *Nature* 373, 257–261.
- Montminy, M. R., Sevarino, K. A., Wagner, J. A., Mandel, G., and Goodman, R. H. (1986) Identification of a cyclic-AMP-responsive element within the rat somatostatin gene. *Proc. Natl. Acad. Sci. U.S.A.* 83, 6682–6686.
- Quinn, P. G., Wong, T. W., Magnuson, M. A., Shabb, J. B., and Granner, D. K. (1988) Identification of basal and cyclic AMP regulatory elements in the promoter of the phosphoenolpyruvate carboxykinase gene. *Mol. Cell. Biol.* 8, 3467–3475.
- Horn, F., Windle, J. J., Barnhart, K. M., and Mellon, P. L. (1992) Tissue-specific gene expression in the pituitary: the glycoprotein hormone alpha-subunit gene is regulated by a gonadotrope-specific protein. *Mol. Cell. Biol.* 12, 2143–2153.
- Sims, S. H., Cha, Y., Romine, M. F., Gao, P. Q., Gottlieb, K., and Deisseroth, A. B. (1993) A novel interferon-inducible domain: structural and functional analysis of the human interferon regulatory factor 1 gene promoter. *Mol. Cell. Biol.* 13, 690–702.
- Kim, Y. J., Pan, H., and Verma, A. K. (1994) Non-AP-1 tumor promoter 12-O-tetradecanoylphorbol-13-acetate-responsive sequences in the human ornithine decarboxylase gene. *Mol. Carcinog.* 10, 169–179.
- Orten, D. J., Strawhecker, J. M., Sanderson, S. D., Huang, D., Prystowsky, M. B., and Hinrichs, S. H. (1994) Differential effects of monoclonal antibodies on activating transcription factor-1 and cAMP response element binding protein interactions with DNA. *J. Biol. Chem.* 269, 32254–32263.
- Evers, B. M., Wang, X., Zhou, Z., Townsend, C. M., Jr., McNeil, G. P., and Dobner, P. R. (1995) Characterization of promoter elements required for cell-specific expression of the neurotensin/neuromedin N gene in a human endocrine cell line. *Mol. Cell. Biol.* 15, 3870–3881.
- Ball, H. J., Shine, J., and Herzog, H. (1995) Multiple promoters regulate tissue-specific expression of the human NPY-Y1 receptor gene. *J. Biol. Chem.* 270, 27272–27276.
- Foulkes, N. S., Borjigin, J., Snyder, S. H., and Sassone-Corsi, P. (1996) Transcriptional control of circadian hormone synthesis via the CREM feedback loop. *Proc. Natl. Acad. Sci. U.S.A.* 93, 14140–14145.
- Guo, B., Stein, J. L., van Wijnen, A. J., and Stein, G. S. (1997) ATF1 and CREB trans-activate a cell cycle regulated histone H4 gene at a distal nuclear matrix associated promoter element. *Biochemistry* 36, 14447–14455.
- Sabbah, M., Courilleau, D., Mester, J., and Redeuilh, G. (1999) Estrogen induction of the cyclin D1 promoter: involvement of a cAMP response-like element. *Proc. Natl. Acad. Sci. U.S.A.* 96, 11217–11222.
- Kim, H. P., Roe, J. H., Chock, P. B., and Yim, M. B. (1999) Transcriptional activation of the human manganese superoxide dismutase gene mediated by tetradecanoylphorbol acetate. *J. Biol. Chem.* 274, 37455–37460.
- Grassl, C., Luckow, B., Schlondorff, D., and Dendorfer, U. (1999) Transcriptional regulation of the interleukin-6 gene in mesangial cells. *J. Am. Soc. Nephrol.* 10, 1466–1477.
- Jessen, B. A., Qin, Q., and Rice, R. H. (2000) Functional AP1 and CRE response elements in the human keratinocyte transglutaminase promoter mediating Wnt suppression. *Gene* 254, 77–85.
- Perillo, B., Sasso, A., Abbondanza, C., and Palumbo, G. (2000) 17beta-estradiol inhibits apoptosis in MCF-7 cells, inducing bcl-2 expression via two estrogen-responsive elements present in the coding sequence. *Mol. Cell. Biol.* 20, 2890–2901.
- Chen, A., Laskar-Levy, O., Ben-Aroya, N., and Koch, Y. (2001) Transcriptional regulation of the human GnRH II gene is mediated by a putative cAMP response element. *Endocrinology* 142, 3483–3492.
- Berhane, K., and Boggaram, V. (2001) Identification of a novel DNA regulatory element in the rabbit surfactant protein B (SP-B) promoter that is a target for ATF/CREB and AP-1 transcription factors. *Gene* 268, 141–151.
- Majumder, S., Varadharaj, S., Ghoshal, K., Monani, U., Burghes, A. H., and Jacob, S. T. (2004) Identification of a novel cyclic AMP-response element (CRE-II) and the role of CREB-1 in the cAMP-induced expression of the survival motor neuron (SMN) gene. *J. Biol. Chem.* 279, 14803–14811.
- Cote-Velez, A., Perez-Martinez, L., Diaz-Gallardo, M. Y., Perez-Monter, C., Carreon-Rodriguez, A., Charli, J. L., and Joseph-Bravo, P. (2005) Dexamethasone represses cAMP rapid upregulation of TRH gene transcription: identification of a composite glucocorticoid response element and a cAMP response element in TRH promoter. *J. Mol. Endocrinol.* 34, 177–197.
- Rani, C. S., Qiang, M., and Ticku, M. K. (2005) Potential role of cAMP response element-binding protein in ethanol-induced N-methyl-D-aspartate receptor 2B subunit gene transcription in fetal mouse cortical cells. *Mol. Pharmacol.* 67, 2126–2136.
- Hartl, M., Karagiannidis, A. I., and Bister, K. (2006) Cooperative cell transformation by Myc/Mil(Raf) involves induction of AP-1 and activation of genes implicated in cell motility and metastasis. *Oncogene* 25, 4043–4055.
- Hamzaoui, H., Rizk-Rabin, M., Gordon, J., Offutt, C., Bertherat, J., and Bouizar, Z. (2007) PTHrP P3 promoter activity in breast cancer cell lines: role of Ets1 and CBP (CREB binding protein). *Mol. Cell. Endocrinol.* 268, 75–84.
- Min, B. W., Kim, C. G., Ko, J., Lim, Y., Lee, Y. H., and Shin, S. Y. (2008) Transcription of the protein kinase C-delta gene is activated by JNK through c-Jun and ATF2 in response to the anticancer agent doxorubicin. *Exp. Mol. Med.* 40, 699–708.
- Seldeen, K. L., McDonald, C. B., Deegan, B. J., and Farooq, A. (2008) Coupling of folding and DNA-binding in the bZIP domains of Jun-Fos heterodimeric transcription factor. *Arch. Biochem. Biophys.* 473, 48–60.
- Cantor, C. R., Warshaw, M. M., and Shapiro, H. (1970) Oligonucleotide interactions. 3. Circular dichroism studies of the conformation of deoxyoligonucleotides. *Biopolymers* 9, 1059–1077.

39. Kwon, H., Park, S., Lee, S., Lee, D. K., and Yang, C. H. (2001) Determination of binding constant of transcription factor AP-1 and DNA. Application of inhibitors. *Eur. J. Biochem.* 268, 565–572.
40. Ryseck, R. P., and Bravo, R. (1991) c-JUN, JUN B, and JUN D differ in their binding affinities to AP-1 and CRE consensus sequences: effect of FOS proteins. *Oncogene* 6, 533–542.
41. Nakabeppu, Y., and Nathans, D. (1989) The basic region of Fos mediates specific DNA binding. *EMBO J.* 8, 3833–3841.
42. Rauscher, F. J., III, Voulalas, P. J., Franza, B. R., Jr., and Curran, T. (1988) Fos and Jun bind cooperatively to the AP-1 site: reconstitution in vitro. *Genes Dev.* 2, 1687–1699.
43. Berger, C., Piubelli, L., Haditsch, U., and Bosshard, H. R. (1998) Diffusion-controlled DNA recognition by an unfolded, monomeric bZIP transcription factor. *FEBS Lett.* 425, 14–18.
44. Halford, S. E., and Marko, J. F. (2004) How do site-specific DNA-binding proteins find their targets? *Nucleic Acids Res.* 32, 3040–3052.
45. Boeger, H., Bushnell, D. A., Davis, R., Griesenbeck, J., Lorch, Y., Strattan, J. S., Westover, K. D., and Kornberg, R. D. (2005) Structural basis of eukaryotic gene transcription. *FEBS Lett.* 579, 899–903.
46. Klenin, K. V., Merlitz, H., Langowski, J., and Wu, C. X. (2006) Facilitated diffusion of DNA-binding proteins. *Phys. Rev. Lett.* 96, 018104.
47. Lumry, R., and Rajender, S. (1970) Enthalpy-entropy compensation phenomena in water solutions of proteins and small molecules: a ubiquitous property of water. *Biopolymers* 9, 1125–1227.
48. Eftink, M. R., Anusiem, A. C., and Biltonen, R. L. (1983) Enthalpy-entropy compensation and heat capacity changes for protein-ligand interactions: general thermodynamic models and data for the binding of nucleotides to ribonuclease A. *Biochemistry* 22, 3884–3896.
49. Cooper, A., Johnson, C. M., Lakey, J. H., and Nollmann, M. (2001) Heat does not come in different colours: entropy-enthalpy compensation, free energy windows, quantum confinement, pressure perturbation calorimetry, solvation and the multiple causes of heat capacity effects in biomolecular interactions. *Biophys. Chem.* 93, 215–230.
50. Sharp, K. (2001) Entropy-enthalpy compensation: fact or artifact? *Protein Sci.* 10, 661–667.
51. Starikov, E. B., and Norden, B. (2007) Enthalpy-entropy compensation: a phantom or something useful? *J. Phys. Chem. B* 111, 14431–14435.
52. Berger, C., Jelesarov, I., and Bosshard, H. R. (1996) Coupled folding and site-specific binding of the GCN4-bZIP transcription factor to the AP-1 and ATF/CREB DNA sites studied by microcalorimetry. *Biochemistry* 35, 14984–14991.
53. Ladbury, J. E., Wright, J. G., Sturtevant, J. M., and Sigler, P. B. (1994) A thermodynamic study of the trp repressor-operator interaction. *J. Mol. Biol.* 238, 669–681.
54. Foguel, D., and Silva, J. L. (1994) Cold denaturation of a repressor-operator complex: the role of entropy in protein-DNA recognition. *Proc. Natl. Acad. Sci. U.S.A.* 91, 8244–8247.
55. Petri, V., Hsieh, M., and Brenowitz, M. (1995) Thermodynamic and kinetic characterization of the binding of the TATA binding protein to the adenovirus E4 promoter. *Biochemistry* 34, 9977–9984.
56. Merabet, E., and Ackers, G. K. (1995) Calorimetric analysis of lambda cI repressor binding to DNA operator sites. *Biochemistry* 34, 8554–8563.
57. Milev, S., Bosshard, H. R., and Jelesarov, I. (2005) Enthalpic and entropic effects of salt and polyol osmolytes on site-specific protein-DNA association: the integrase Tn916-DNA complex. *Biochemistry* 44, 285–293.
58. Koo, H. S., Wu, H. M., and Crothers, D. M. (1986) DNA bending at adenine-thymine tracts. *Nature* 320, 501–506.
59. Alexeev, D. G., Lipanov, A. A., and Skuratovskii, I. (1987) Poly-(dA)·poly(dT) is a B-type double helix with a distinctively narrow minor groove. *Nature* 325, 821–823.
60. Arnott, S., Chandrasekaran, R., Hall, I. H., and Puigjaner, L. C. (1983) Heteronomous DNA. *Nucleic Acids Res.* 11, 4141–4155.
61. Nelson, H. C., Finch, J. T., Luisi, B. F., and Klug, A. (1987) The structure of an oligo(dA)·oligo(dT) tract and its biological implications. *Nature* 330, 221–226.
62. Coll, M., Frederick, C. A., Wang, A. H., and Rich, A. (1987) A bifurcated hydrogen-bonded conformation in the d(A·T) base pairs of the DNA dodecamer d(CGCAAATTTGCG) and its complex with distamycin. *Proc. Natl. Acad. Sci. U.S.A.* 84, 8385–8389.
63. DiGabriele, A. D., Sanderson, M. R., and Steitz, T. A. (1989) Crystal lattice packing is important in determining the bend of a DNA dodecamer containing an adenine tract. *Proc. Natl. Acad. Sci. U.S.A.* 86, 1816–1820.
64. Kerppola, T. K., and Curran, T. (1993) Selective DNA bending by a variety of bZIP proteins. *Mol. Cell. Biol.* 13, 5479–5489.
65. Leonard, D. A., Rajaram, N., and Kerppola, T. K. (1997) Structural basis of DNA bending and oriented heterodimer binding by the basic leucine zipper domains of Fos and Jun. *Proc. Natl. Acad. Sci. U.S.A.* 94, 4913–4918.
66. Leonard, D. A., and Kerppola, T. K. (1998) DNA bending determines Fos-Jun heterodimer orientation. *Nat. Struct. Biol.* 5, 877–881.
67. Rowntree, R., and Harris, A. (2002) DNA polymorphisms in potential regulatory elements of the CFTR gene alter transcription factor binding. *Hum. Genet.* 111, 66–74.
68. Wiseman, T., Williston, S., Brandts, J. F., and Lin, L. N. (1989) Rapid measurement of binding constants and heats of binding using a new titration calorimeter. *Anal. Biochem.* 179, 131–137.